Construction of Novel Brain-Targeting Gene Delivery System by Natural Magnetic Nanoparticles

Lei Han,[1,2] Anling Zhang,[2] Hanjie Wang,[1] Peiyu Pu,[2] Chunsheng Kang,[2] Jin Chang[1]

[1]*Institute of Nanobiotechnology, School of Materials Science and Engineering, Tianjin University, and Tianjin Key Laboratory of Composites and Functional Materials, Tianjin 300072, China*
[2]*Department of Neurosurgery, Laboratory of Neuro-Oncology, Tianjin Medical University General Hospital, Key Laboratory of Neurotrauma, Variation and Regeneration, Ministry of Education and Tianjin Municipal Government, Tianjin 300052, China*

Received 26 August 2010; accepted 17 December 2010
DOI 10.1002/app.33995
Published online 12 April 2011 in Wiley Online Library (wileyonlinelibrary.com).

ABSTRACT: The main objective in gene therapy of brain tumors is to develop efficient, low toxic, and brain-targeting gene delivery systems which can cross the blood-brain barrier (BBB) and deliver therapeutic gene to the brain cancerous tissues. In this study, we designed and constructed a novel gene delivery systems (Tat-MS-PAMAM) by modifying the magnetosome (MS) with polyamidoamine (PAMAM) dendrimers and Tat peptides for the first time. Tat-MS-PAMAM readily formed polyplexes with the luciferase reporter plasmid (pGL-3) and improved plasmid complexation and stability against polyanion and DNase I. Transfection efficiencies of Tat-MS-PAMAM polyplexes with pGL-3 were studied using U251 human glioma cells *in vitro*. The result showed that the incorporation of external magnetic field and Tat peptides could significantly improve transfection efficiency of delivery system. Furthermore, biodistribution *in vivo* demonstrated that Tat-MS-PAMAM could efficiently transport across the BBB and assemble at brain tissue of rat detected by single photo emission computed tomography. Thus, with the multifunction of magnetic targeting, BBB transporting, and efficient gene transfecting, Tat-MS-PAMAM might be a novel nonviral delivery system for gene therapy of brain tumors. © 2011 Wiley Periodicals, Inc. J Appl Polym Sci 121: 3446–3454, 2011

Key words: targeted gene delivery system; magnetosome; glioma; transmembrane; biodistribution

INTRODUCTION

There is currently a great deal of interest in the therapeutic application of gene on brain tumors.[1] Gene therapy of brain tumors has remained two of the most challenging aspects of gene delivery due to the impermeable nature of the blood-brain barrier (BBB)[2] and the lack of tumor tissue specificity.[3] One approach to overcome these two difficulties involves the construction of magnetic delivery system with the transmembrane function for the site-specific delivery of gene to brain tissue by the external magnetic field after across the BBB. Magnetic delivery system offers advantages over conventional delivery system in terms of the ability to localize the gene at tumor tissue and limit systemic distribution.[4] Recently, a new natural magnetic nanoparticles with controlled size (40–120 nm) and better biocompatibility, called magnetosome (MS), was found in the magnetotactic bacteria.[5] The MS was consisted of magnetic core enveloped by stable lipid membrane that contained some lipids and proteins. It has been used as the magnetic vectors for the antibody[6] and drug.[7] However, no reports are closely associated with use of MS as gene-loaded vectors for brain tumor therapy.

Polyamidoamine (PAMAM) with highly ordered structure is one kind of good nonviral vectors because of the advantages of safety, simplicity of use, and ease of mass production compared with viral vectors with an inherent risk for clinical use.[8] But, PAMAM cannot deliver the gene across the BBB to the brain tissue by itself. In recent years, strategies have been developed to overcome the BBB and cellular membranes. One approach is to link the polyplexes of gene and vector to the specific small regions of transactivating transcriptional activator protein (Tat) derived from the HIV-1. The use of

Correspondence to: C. Kang or J. Chang (jinchang@tju.edu.cn or kang97061@yahoo.com).

Contract grant sponsor: National Natural Science Foundation of China; contract grant number: 50873076.
Contract grant sponsor: Program for New Century Excellent Talents in University; contract grant number: NCET-07-0615.
Contract grant sponsors: Key Project Foundation from Tianjin Science and Technology Committee; contract grant numbers: No.09ZCGYSF00900, 09JCZDJC17600.
Contract grant sponsor: Tianjin Public Health Bureau (Technology Fund); contract grant number: 09KZ112

such peptide for drug or gene delivery across cellular membranes and BBB is getting increased attention.[9,10]

In this article, we fully used the advantages of MS, PAMAM, and Tat peptides to solve two problems associated with gene therapy of brain tumor mentioned above by construction nanoscale magnetic gene delivery system composed of MS covered with PAMAM and Tat peptides (Tat-MS-PAMAM) for the first time. These results showed that Tat-MS-PAMAM might be a novel delivery system with the transmembrane ability for delivery of gene to the brain tissue.

EXPERIMENTAL PROCEDURE

Materials

Magnetosomes, which were isolated from the cells of M *Magnetospirillum gryphiswaldense* MSR-1, were kindly presented by Professor Ying Li (Microbiology Department, College of Biological Sciences, China Agricultural University). PAMAM G3.0 was kindly presented by Professor Xinru Jia (College of Chemistry, Peking University). Human glioblastoma U251-MG cells were obtained from Institute of Biochemistry and Cell Biology, Chinese Academy of Science. Cells were cultured in Dulbecco's modified Eagle's medium supplemented with 10% heat-inactivated fetal calf serum, 4 mM glutamine, 50 units/mL penicillin, and 50 μg/mL streptomycin. (1-ethyl-3-[3-dimethylaminopropyl]carbodiimidehydrochloricde) (EDC), sulfosuccinimidyl6-[3′(2-pyridyldithio)-propionamido]hexanoate (Sulfo-LC-SPDP) were purchased from Pierce (Rockford, IL). Luciferase plasmid (pGL-3) with 4818bp was used as the reporter gene in this study. Luciferase assay system was obtained from Promega. Lipofectamine 2000 was purchased from Invitrogen. A modified Tat peptide with a sequence CGRKKRRQRRRK was synthesized by SANGON BIO.BASIC. INC. (Shanghai, China). All other chemicals were of analytical grade.

Modification of MS with PAMAM and Tat peptide

The Modification of MS with PAMAM was carried out using zero-length crosslinker, EDC HCL. At first, 1 mL of PAMAM ultrapure water solution (2 mg/mL) was added to 1mL of MS 0.1*M* MES buffer (1 mg/mL, pH = 7.4). After incubation MS with PAMAM for 20 min, 10 mg EDC HCL dissolved in ultrapure water was immediately added to above complex solution. The suspension was then dispersed by sonication and incubated for 2 h at room temperature. After reaction, MS-PAMAM was magnetically separated from reaction mixture using a Nd-B magnet washed with phosphate buffered saline (PBS) three times to remove excess EDC HCL, PAMAM, and byproducts.

The conjugation of Tat peptides onto MS-PAMAM was carried out using heterobifunctional coupling reagents, Sulfo-LC-SPDP. At first, 1.0 mg Sulfo-LC-SPDP was added to 1 mL MS-PAMAM suspension (1 mg/mL). The suspension was then dispersed by sonication and incubated for 2 h at room temperature. After the incubation, the Sulfo-LC-SPDP-modified MS-PAMAM was magnetically separated from reaction mixture using a Nd-B magnet and washed three times with PBS. On the other hand, Tat peptide (5.0 mg) was dissolved in PBS and then added to Sulfo-LC-SPDP-modified MS-PAMAM solution. The complexes solution was incubated for 12 h at 4°C. Tat-MS-PAMAM was washed with PBS three times to remove excess Tat peptides.

Characterization of MS-*PAMAM and Tat-MS-PAMAM*

The Fourier transform infrared (FT-IR) spectrum and X-ray photoelectron spectra of MS and MS-PAMAM were recorded on a Bio-Rad FTS 6000 spectrophotometer and Perkin–Elmer PHI1600 ESCA system respectively. The average number of Tat peptide conjugated on the surface of MS-PAMAM was determined by a P2T method.[11] The morphologies of MS, MS-PAMAM and Tat-MS-PAMAM were observed using a JEOL-100CXII TEM. Magnetic property measurement of MS, MS-PAMAM, and Tat-MS-PAMAM were performed by a vibrating sample magnetometer from LakeShore.

Polyplex formation and stability assay

Agarose gel electrophoresis studies and zeta potential analysis

Polyplexes were formed at different mass ratios between the nanoparticles (MS-PAMAM or Tat-MS-PAMAM) and pGL-3 plasmid. Each sample was then analyzed by electrophoresis and the resulting gel was then photographed with a UVP gel documentation system.[12] The surface charge of the polyplexes was determined by measuring zeta potential values via the Malvern Zetasizer 3000Has system (Malvern Instruments, UK) using the PCS 1.61 software. The mean values and the corresponding standard deviation (SD) were calculated in three independent measurements, six runs each.

Polyplex stability against heparin and DNase I

Stability of polyplexes, MS-PAMAM/pGL-3 and Tat-MS-PAMAM/pGL-3, was studied in the presence of heparin and DNase I *in vitro*.[13] Polyplexes, MS-PAMAM/pGL-3 and Tat-MS-PAMAM/pGL-3, were

prepared at mass ratio of 20 : 1 and 12.5 : 1, respectively, in 5% glucose using 20 μg pGL-3 plasmid in a total volume of 100 μL. Increasing amounts of heparin in 10 μL pure water were added to 100 μL polyplexes solution, yielding heparin concentrations of 0.1–2.0 IU per microgram plasmid, and incubated for 10 min at 37°C. Twenty-five microliters of this mixture was applied to the 1% agarose gel. The resulting gel was visualized and photographed with a UVP gel documentation system.

Polyplexes were prepared as above described. Aliquots of 5 μL corresponding reverse fluponding to 1 μg of plasmid were incubated with 0.01, 0.1, 1, 2.5, and 5 IU of DNase I in 1 μL digestion buffer for 15 min at 37°C. To stop the DNase I digestion, 6 μL termination buffer were added, followed by 2 μL of a heparin solution containing 1000 IU per milliliter to separate the plasmid from polyplexes. The resulting mixtures were applied to the 1% agarose gel. The resulting gel was visualized and photographed with a UVP gel documentation system.

Cytotoxicity assay *in vitro*

For the cytotoxicity of MS-PAMAM and Tat-MS-PAMAM assay *in vitro*, the colorimetric MTT assay was performed.[14] Briefly, U251 cells were seeded at a density of 0.5×10^4 cells/well in a 96-well plate and grown in 100 μL of the Dulbecco's modified Eagle's medium (DMEM) supplemented with 10% FBS for 1 day before incubation with different concentrations of nanoparticles (MS-PAMAM, Tat-MS-PAMAM, and Lipofectamine 2000). After treating cells with nanoparticles for 48 h, 25 μL of MTT solution (5 mg/mL) was added to each well and incubated further for 4 h. The media was removed and 150 μL of dimethyl sulfoxide (DMSO) was added and the absorbance was measured at 570 nm using a microplate reader. Each test was repeated in eight wells.

Transfection experiments *in vitro*

The transfection efficiency of MS-PAMAM and Tat-MS-PAMAM in U251 cells was evaluated by using the pGL-3 reporter plasmid. Before transfection, the U251 cells were seeded to a 96-well plate at a density of 0.5×10^4 cells/well with 100 μL of the completed DMEM per well. The cells were then cultured for 24 h period to obtain 80–90% confluence. For transfection with pGL-3 plasmid, the culture medium was replaced with 100 μL of serum-free medium and transfection was carried out by adding an aliquot of 50 μL of either MS-PAMAM/pGL-3 or Tat-MS-PAMAM/pGL-3 polyplexes at different mass ratio containing 100 ng of pGL-3 plasmid into each well of the 96-well plate. A total of 100 ng pGL-3 plasmid/well was complexed to the Lipofectamine 2000 and transfection process according to the manufacturer's protocol as the positive control. Each transfection test was repeated in eight wells. The cell culture plate was placed on a Nd-B permanent magnet, which led to a magnetic flux density of 250 mT and a magnetic field gradient perpendicular to the well plate of 10 T/m in the area of the cells. After incubated with the cells for 4 h, the medium was replaced with the DMEM supplemented with 10% FBS and the cells were further incubated for another 48 h. Each transfection test was repeated without the magnetic field effect at the same condition.

For luciferase assay, the growth medium was removed and the cells were washed by 200 μL PBS and then lysed using 200 μL reporter lysis buffer. After two cycles of freezing and thawing, the solution was transferred into microtubes and centrifuged for 3 min. Luciferase activity of the supernatants was measured using 100 μL of luciferase assay reagent (Promega) on a luminometer (Berthold) for 30 s. The light units were normalized against protein concentration in the cell extracts. The total protein was measured according to a bicinchoninic acid (BCA) protein assay kit (Pierce) and luciferase activity was reported in terms of relative light unit (RLU)/mg cellular protein. Data were shown as mean ± SD based on two independent measurements.

Biodistribution assay *in vivo*

Radiolabeling of MS-PAMAM and Tat-MS-PAMAM

The radiolabeling of MS-PAMAM and Tat-MS-PAMAM nanoparticles was performed using the method reported by Yuan et al.[15] Nanoparticles (2 mg/mL) were dispersed in Tris–HCl buffer (pH = 7.2). Nitrogen purging, before mixing was carried out to degas all solutions. To 0.1 mL ^{99m}Tc (5.2 mCi) in saline, 5 mg of solid sodium borohydride was added directly with continuous stirring followed by immediate addition of the nanoparticles buffer. The solution was stirred for 20 min at room temperature, then centrifugated at 18,000 rpm for 10 min followed by washing three times with buffer under sonication condition. The labeling efficiency of ^{99m}Tc to nanoparticle was assessed by the eq. (1).

$$\text{Labeling efficiency}\,\% = \text{Total counts} - \text{counts of free pertechnetate}/\text{Total counts} \quad (1)$$

Stability study of ^{99m}Tc-MS-PAMAM and ^{99m}Tc-Tat-MS-PAMAM

The stability of the ^{99m}Tc-MS-PAMAM and ^{99m}Tc-Tat-MS-PAMAM nanoparticles was determined *in vitro* by γ-counter.[16] A total of 500 μg of ^{99m}Tc-

MS-PAMAM or ^{99m}Tc-Tat-MS-PAMAM nanoparticle solution (1 mg/mL) in Tris–HCL buffer (pH = 7.2) was incubated at 37°C for 4 h. After magnetic separation, the radioactivity of supernatant solution was counted by γ-counter to assess the stability of the polyplexes.

Biodistribution of MS-PAMAM and Tat-MS-PAMAM

The biodistribution and the ability for crossing BBB of ^{99m}Tc-MS-PAMAM and ^{99m}Tc-Tat-MS-PAMAM nanoparticles were studied in 6–8-week-old male SD rats by single photo emission computed tomography [SPECT (GE DISCOVERY-VH, USA)] images analysis. After injection of 100 μL ^{99m}Tc-MS-PAMAM or ^{99m}Tc-Tat-MS-PAMAM nanoparticle solution (1 mg/mL) by carotid artery, the anesthetized rats were placed ventrally on a platform so that the head was centered between the poles of the magnet for different time intervals, and the magnetic field strength at the midpoint of the air gap was 1T. The image was divided into five regions of interest, which were brain, heart and lung, liver and spleen, kidney, and bladder, respectively. The radioactivity in each region was counted by SPECT images analysis and expressed as percent injected dose per organ. Each test was repeated in triplicates.

RESULTS AND DISCUSSION

Characterization of Tat-MS-PAMAM

The conjugation of MS with PAMAM was confirmed by analysis of FT-IR and X-ray photoelectron spectroscopy (XPS). The FT-IR spectra [Fig. 1(a)] showed that, compared with the MS, the MS-PAMAM nanoparticles possessed more intensive absorption band at 3310 cm^{-1} due to the bending vibration of the —NH_2 group, absorption bands at 1732, 1650, 1550, 1460 cm^{-1} due to the —CO—NH— group, and the characteristic absorption band of the Fe—O bond of magnetite was in 579 cm^{-1}. All these revealed the existence of PAMAM on the surface of MS. The incorporation of PAMAM to the surface of MS was also confirmed by XPS spectroscopy [Fig. 1(b,c)]. Element analysis results showed that the nitrogen element content of MS-PAMAM was higher than that of MS because of the incorporation of PAMAM on the MS surface. Typical C1s XPS spectra of MS and MS-PAMAM were attributed. The C1s peak of carboxyl groups in the MS-PAMAM disappeared for they were used to conjugated with PAMAM. At the same time, the C—C bond percent content was increased in the MS-PAMAM than that of MS for the incorporation of organic compound, PAMAM. In addition to the peaks of C1s, there was an additional N1s peak of MS and MS-PAMAM on the XPS spectrum, which could be possibly deconvoluted as four areas: the 399 eV peak was associated with peptide bond units. The 401 eV peak was for the amidocyanogen amine units. In contrast, after conjugating of the PAMAM on the surface of MS, the 401 eV peak was disappeared since the amount of peptide bond was increased largely. There were large amount of peptide bonds in the PAMAM structure, therefore incorporation of PAMAM on the surface of MS largely increased the amounts of peptide bond of the MS-PAMAM. It could be concluded that the PAMAM was successfully conjugated on the surface of the MS by FT-IR and XPS analysis. To determine average number of Tat peptide conjugated on the surface of MS-PAMAM, a P2T method was adopted.[17,18] Measuring the specific absorption of the released pyridine-2-thione at 343 nm, an average of 3190 Tat peptides were attached per MS-PAMAM nanoparticle, assuming 1938582 Fe atoms per MS.[19]

As shown in Figure 1(d), it could be seen that the morphology of MS, MS-PAMAM, and Tat-MS-PAMAM was close to spherical with dimension about 50 nm. They showed excellent dispersivity and arranged in bent chains which tend to form closed loops in suspension so as to minimize their magnetic stray field energy.[20] However, it was not easy to directly observe PAMAM and Tat peptide coating layer on the MS surface from transmission electron micrograph (TEM) because they were transparent for TEM observation.[21] The excellent dispersivity of MS-PAMAM and Tat-MS-PAMAM also implied the repulsive force by ionic repulsion from amine of PAMAM and Tat peptide.[22] From the magnetization versus field curve for MS, MS-PAMAM, and Tat-MS-PAMAM [Fig. 1(e)], both MS-PAMAM and Tat-MS-PAMAM exhibited ferromagnetic behavior for their magnetic core, MS was ferromagnetic.[23] The saturation magnetization of the MS, 71.47 emu/g, was larger than that of MS-PAMAM, 65.74 emu/g and Tat-MS-PAMAM, 62.45 emu/g in the field region of ±1T at 300 K. This was due to the presence of PAMAM and Tat peptide of 3–5 nm thickness on the surface of MS. At the same time, the results showed that both MS-PAMAM and Tat-MS-PAMAM had high magnetic response due to perfect crystallinity of MS. The characterization above demonstrated that the nanoscale gene delivery system with the magnetic targeting and transmembrane functions, Tat-MS-PAMAM, was successfully constructed.

Reporter gene transfection assay *in vitro*

Agarose gel electrophoresis studies

To assess the formation of MS-PAMAM/pGL-3 and Tat-MS-PAMAM/pGL-3 polyplexes, gel electrophoresis of the polyplexes was performed at

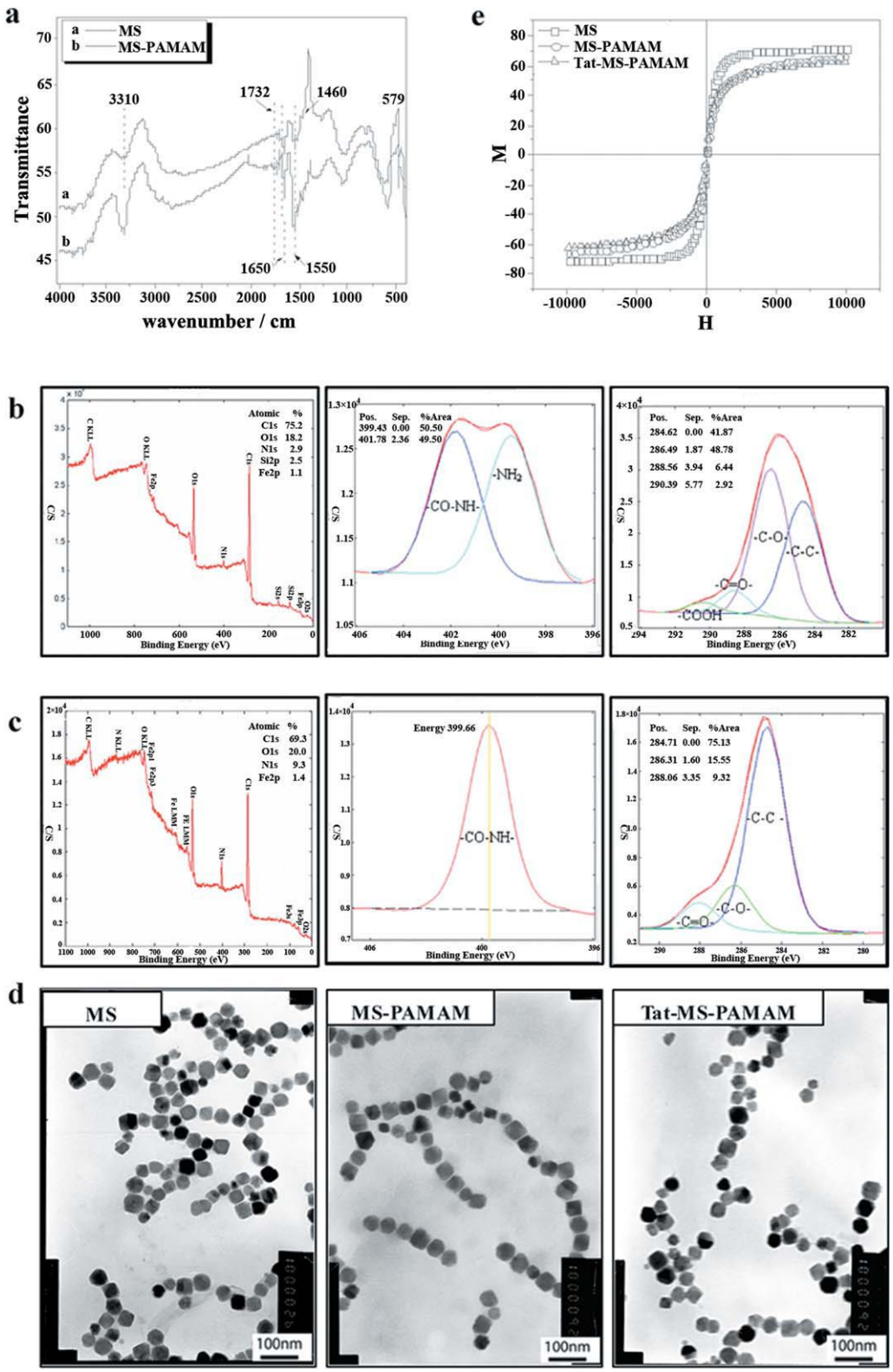

Figure 1 Construction and characterization of MS-PAMAM and Tat-MS-PAMAM. (a) FT-IR spectra of MS and MS-PAMAM. (b, c) High-resolution XPS spectra of MS and MS-PAMAM. (d) TEM images of MS, MS-PAMAM and Tat-MS-PAMAM. The scale bars in all photographs represent 100 nm. (e) Magnetic properties of MS, MS-PAMAM and Tat-MS-PAMAM were analyzed by magnetization curve obtained by VSM at room temperature. [Color figure can be viewed in the online issue, which is available at wileyonlinelibrary.com.]

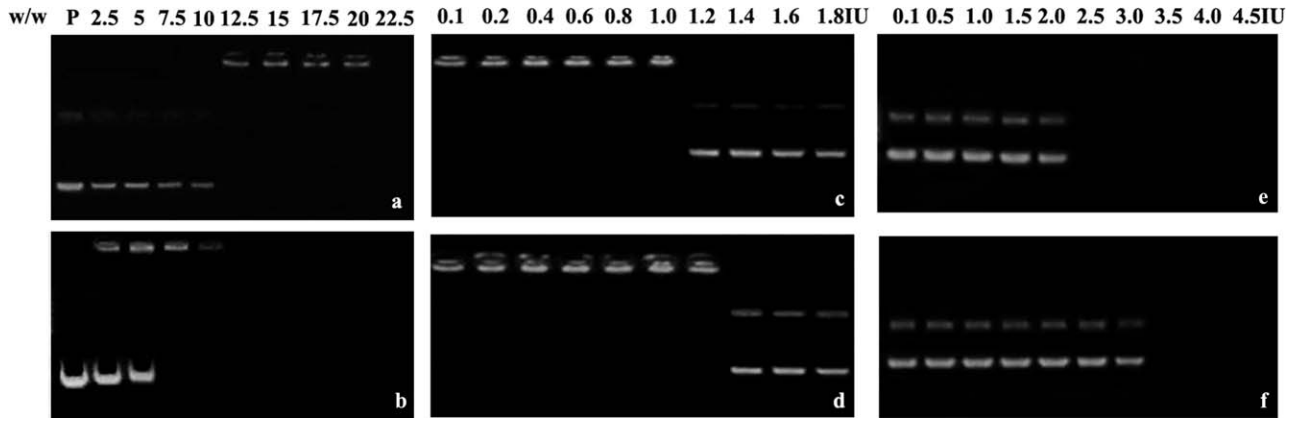

Figure 2 Agarose gel electrophoreses assay. Electrophoretic mobility of pGL-3 plasmid in the polyplexes of MS-PAMAM (a) or Tat-MS-PAMAM (b) with pGL-3 plasmid at various mass ratios (2.5 : 1, 5 : 1, 7.5 : 1, 10 : 1, 12.5 : 1, 15 : 1, 17.5 : 1, 20 : 1, 22.5 : 1). MS-PAMAM/pGL-3 (c) and Tat-MS-PAMAM/pGL-3 (d) polyplexes challenged with increasing amounts of heparin (0.1, 0.2, 0.4, 0.6, 0.8, 1.0, 1.2, 1.4, 1.6, 1.8 IU heparin per microgram plasmid). MS-PAMAM/pGL-3 (e) and Tat-MS-PAMAM/pGL-3 (f) polyplexes challenged with increasing amounts of DNase I (0.1, 0.5, 1.0, 1.5, 2.0, 2.5, 3.0, 3.5, 4.0, 4.5 IU DNase I per microgram plasmid).

different mass ratios of nanoparticles and pGL-3. As shown in Figure 2(a,b), the pGL-3 plasmid showed complete retardation at a mass ratio of 1 : 12.5 with MS-PAMAM and 1 : 7.5 with Tat-MS-PAMAM. The results showed that Tat-MS-PAMAM with more primary amines was more effective at forming complete polyplexes with pGL-3 than MS-PAMAM.

Polyplexes stability assay

To further investigate whether the enhanced condensation ability of Tat-MS-PAMAM also enhanced the protection of the complexed plasmid against polyanion exchange and enzymatic degradation *in vivo* environment, the polyplex stability was studied in the presence of heparin and DNase I.[24] The polyplexes were challenged with increasing amounts of the polyanion model, heparin. As shown in Figure 2(c), MS-PAMAM could protect plasmid against heparin exchange up to 1.0 IU heparin per microgram plasmid. An amount of 1.2 IU heparin per microgram plasmid resulted in a release of the pGL-3 from the MS-PAMAM/pGL-3 polyplexes. In contrast, as shown in Figure 2(d), Tat-MS-PAMAM was able to complex plasmid up to 1.2 IU heparin without any minor release. And 1.4 IU heparin per microgram plasmid was necessary to completely release the plasmid from these polyplexes, indicating enhanced plasmid condensation ability. Representative images of the DNase I digestion assay were shown in Figure 2(e,f). When Tat-MS-PAMAM/pGL-3 polyplexes were incubated with increasing concentrations of DNase I over a period of 30 min, plasmid digestion occurred at a concentration of 3.0 IU DNase I per microgram plasmid. In the case of MS-PAMAM/pGL-3 polyplexes, plasmid degradation was observed at a significantly lower enzyme concentration (2.5 IU DNase I per microgram plasmid). Compared with MS-PAMAM/pGL-3, the stability of Tat-MS-PAMAM/pGL-3 polyplexes was significantly higher in the presence of high concentration of heparin and DNase I. The higher positive charge density of the Tat-MS-PAMAM could explain this difference.[25]

Zeta potential analysis

The zeta potential of the nanoparticles and polyplexes was determined to quantify their surface charge.[26] The results showed [Fig. 3(a)] that MS displayed negative potential of -20 mV at pH 7.0 due to the abundant hydroxyl and carboxy groups. After MS were modified with PAMAM and Tat peptide, zeta potential of Tat-MS-PAMAM increased to $+$ 35 mV at pH 7.0 due to the incorporation of positive charged PAMAM and Tat peptide on the MS surface, which was higher than that of MS-PAMAM. There is a statistical difference between surface charge of nanoparticles and polyplexes ($P < 0.05$), which showed that lots of positive charges on the surface of nanoparticles bind with negative charges of pGL-3 to form polyplexes. Positively charged polyplexes will be easily attached to negatively charged cell membrane to improve the endocytosis, so the positively charged polyplex is very important for cellular internalization and higher gene delivery efficiency.[22]

Cytotoxicity assay in vitro

The cytotoxicity of nanoparticle will impair their clinical utility as the gene carrier.[27] As presented in Figure 3(b), we compared the cytotoxicity of Lipofectamine 2000 with that of MS-PAMAM and Tat-

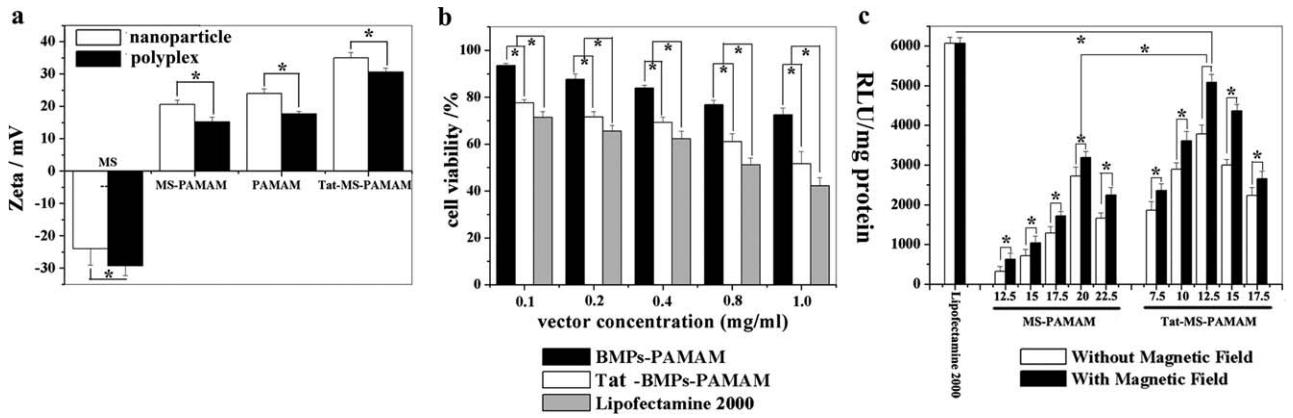

Figure 3 Reporter gene transfection assay *in vitro*. (a) Zeta potential analysis of vectors (MS, PAMAM, MS-PAMAM, and Tat-MS-PAMAM) and polyplexes (mass ratio MS : pGL-3 = 12 : 1, PAMAM : pGL-3 = 0.7 : 1, MS-PAMAM : pGL-3 = 12.5 : 1, Tat-MS-PAMAM : pGL-3 = 7.5 : 1). (b) Cytotoxic effects of the MS-PAMAM, Tat-MS-PAMAM and Lipofectamine 2000 at concentration of 0.1, 0.2, 0.4, 0.8, and 1.0 mg/mL on U251 cells for 48 h were determined by MTT assay. (c) MS-PAMAM, Tat-MS-PAMAM and Lipofectamine 2000 mediated pGL-3 plasmid transfection of U251 cells *in vitro* at different mass ratios (vector/plasmid) in the presence or absence of magnetic field. *Indicates statistically significant difference ($P < 0.05$).

MS-PAMAM. The results showed that although Tat-MS-PAMAM showed slightly increased cytotoxicity compared with MS-PAMAM, both MS-PAMAM and Tat-MS-PAMAM had better biocompatibility than Lipofectamine 2000. We presumed that if MS-PAMAM or Tat-MS-PAMAM could exert a higher level transfection efficiency than, or at least as much as, that of Lipofectamine 2000, MS-PAMAM or Tat-MS-PAMAM should be more promising gene delivery system for possible *in vitro* and *in vivo* transport applications.

Transfection experiment in vitro

The transfection efficiency of MS-PAMAM and Tat-MS-PAMAM were assessed using pGL-3 as reporter gene in U251 cell line *in vitro* because the cells would be used as the therapeutic model in the next step. First, to optimize transfection efficiency of MS-PAMAM and Tat-MS-PAMAM, transfection experiments were performed and compared at various mass ratios for nanoparticles with pGL-3 plasmid. The transfection results [Fig. 3(c)] showed that the maximum transfection efficiency was detected at a mass ratio of 20 : 1 for MS-PAMAM to pGL-3 and 12.5 : 1 for Tat-MS-PAMAM to pGL-3 with external magnetic field. The maximum transfection efficiency of Tat-MS-PAMAM was usually over as 83% as that of Lipofectamine 2000. Second, to further investigate the impact of magnetic field on transfection efficiency, the magnetic field of 250 mT was employed during the transfection assay. It was shown that for each mass ratio tested, a significant improvement in transfection efficiency was observed compared with that without permanent magnetic field ($P < 0.05$). These results indicated that magnetic gene delivery system might deliver plasmid to the cells surface more rapidly and leads to high gene delivery system accumulation on the target cell, which would lead to enhanced uptake into the cell cross the cell membrane and thus yield efficient transgene expression.[28] Third, through comparison peak transfection efficiency of MS-PAMAM and Tat-MS-PAMAM, the results showed that a significant improvement in transfection efficiency was observed with Tat-MS-PAMAM compared with MS-PAMAM ($P < 0.05$), suggesting that covalent coupling of Tat peptide to MS-PAMAM led to facilitate polyplexes interaction with the cell membrane and mediating efficient gene delivery into the cells.[29] The higher gene delivery efficiency and enhanced plasmid condensation as well as the protection function *in vitro* by Tat-MS-PAMAM compared with MS-PAMAM suggested that Tat peptide was involved in both the plasmid compaction process and the cell uptake.[30] But the mechanism of the Tat peptide-mediated uptake was still under discussion.[31]

Biodistribution assay *in vivo*

The transfection assay of the reporter plasmid *in vitro* demonstrated that the Tat-MS-PAMAM could efficiently transfer the gene into cells with the functions of external magnetic field and Tat peptide. Moreover, we had demonstrated that Tat-BMPs-PAMAM complexed with psiRNA targeting the EGFR gene could inhibit U251 cells growth and invasion *in vitro* and *in vivo*.[32] The functions of magnetic targeting and transmembrane of Tat-MS-PAMAM *in vivo* were further analyzed by the radiotracer labeling and SPECT method. About 80–85% of ^{99m}Tc was found to form complexes with the MS-PAMAM and Tat-MS-PAMAM nanoparticles and labeled nanoparticle complexes were found stable up

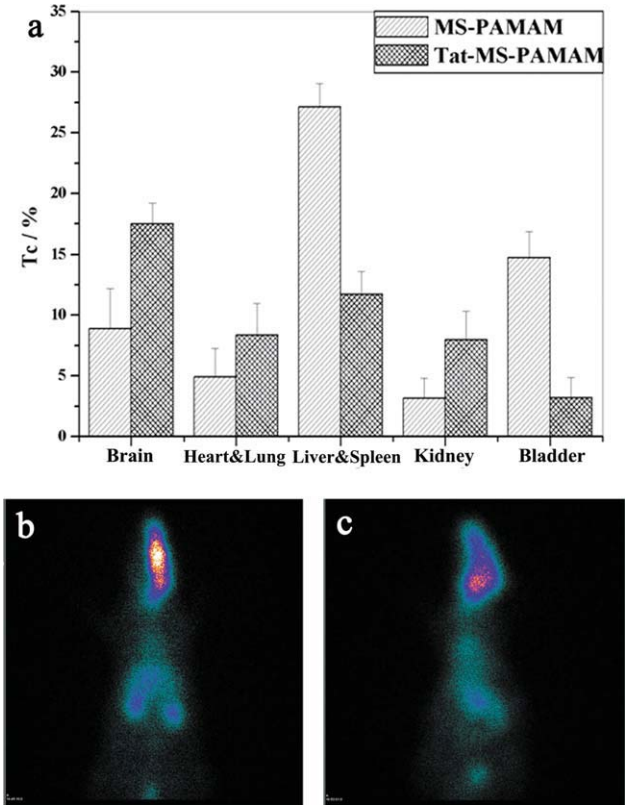

Figure 4 Biodistribution assay *in vivo* by SPECT method. (a) Biodistribution of ^{99m}Tc-MS-PAMAM and ^{99m}Tc-Tat-MS-PAMAMin the body of SD rat ($n = 3$) by carotid injection under magnetic field (1T) for 25 min. The images of the rat injected with ^{99m}Tc-Tat-MS-PAMAM (b) and ^{99m}Tc-MS-PAMAM (c) measured by SPECT. [Color figure can be viewed in the online issue, which is available at wileyonlinelibrary.com.]

to 80–85% in the first 4 h. Figure 4(a) showed the biodistribution of ^{99m}Tc-Tat-MS-PAMAM and ^{99m}Tc-MS-PAMAM in rats whose brain were placed under the magnetic field (1T) for 25 min. The main aim of this study was to test the effect of Tat peptide on the MS-PAMAM crossing the BBB. The radiotracers intensity of ^{99m}Tc-Tat-MS-PAMAM [Fig. 4(b)] in the rat brain was two times that of ^{99m}Tc-MS-PAMAM [Fig. 4(c)]. This may be to the strong transmembrane ability of Tat peptide.[33] Figure 5(a) showed the biodistribution of ^{99m}Tc-Tat-MS-PAMAM in rats whose brain were placed under the magnetic field (1T) for 5, 25 min and placed without the magnetic field for 5, 25 min, respectively. The main aim of this study was to test the magnetic targeting function of the Tat-MS-PAMAM *in vivo*. It was shown that the intensity of radiotracers in the rat's brain was slower decreased with the extending of magnetic field action time [Fig. 5(b,c)] than that without magnetic field [Fig. 5(d,e)]. At the end of 25 min, the intensity of radiotracers in the rat brain which was placed under magnetic field was 1.88-fold higher than that in the rat's brain which was placed without magnetic field. Increasing the magnetic field action time enhanced the action time of magnetic force at the rat's brain so that the Tat-MS-PAMAM could be localized at the rat's brain. The biodistribution results showed that Tat-MS-PAMAM had high magnetic targeting and transmembrane function *in vivo*.

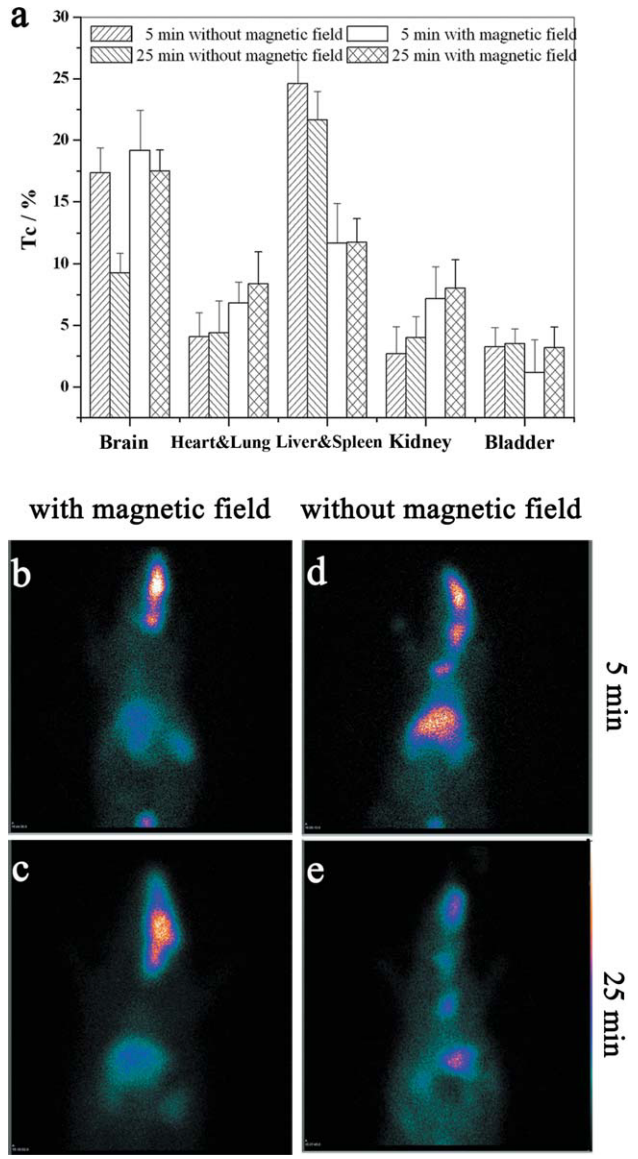

Figure 5 Biodistribution assay *in vivo* by SPECT method. (a) Biodistribution of ^{99m}Tc-Tat-MS-PAMAMin the body of SD rat ($n = 3$) by carotid injection without magnetic field for 5 min, 25 min or with magnetic field (1T) on its brain for treatment time of 5 min, 25 min. The images of the rat injected with ^{99m}Tc-Tat-MS-PAMAM by carotid injection with magnetic field (1T) for 5 min (b), 25 min (c) or without magnetic field on its brain for treatment time of 5 min (d), 25 min (e) measured by SPECT. [Color figure can be viewed in the online issue, which is available at wileyonlinelibrary.com.]

CONCLUSIONS

In conclusion, natural magnetic nanoparticles formed by biomineralization, MS, the surface of which was anchored with PAMAM macromolecules and Tat peptides, had been successfully synthesized for brain-targeting gene delivery across the BBB for the first time. Tat-MS-PAMAM with good cytocompatibility could combine with pGL-3 to form stable polyplexes in polyanion and DNase I environment via electrostatic means and could efficiently transfect pGL-3 into U251 cells *in vitro*. The biodistribution assay *in vivo* demonstrated that Tat-MS-PAMAM could reach the rat brain across the BBB via the conjunct functions of the external magnetic field and Tat peptide. The results of transfection assay *in vitro* and biodistribution assay *in vivo* showed that Tat-MS-PAMAM with high transfection efficiency could efficiently stride over BBB and accurately assemble at brain tissue guided by external magnetic field. The magnetic targeting ability and Tat peptide-mediated crossing the BBB function make this delivery system attractive to complement and improve existing treatment methods for brain tumors therapy.

The authors thank Professor Ying Li (China Agricultural University) for presenting magnetosomes and Professor Xinru Jia (Peking University of China) for presenting polyamidoamine dendrimer.

References

1. Germano, I. M.; Binello, E. J Neurooncol 2009, 1, 79.
2. Orive, G; Ali, O.; A; Anitua, E; Pedraz, J. L.; Emerich, D. F. Biochim Biophys Acta 2010, 1, 96.
3. Westphal, M.; Lamszus, K. Recent Results Canc Res 2009, 171, 155.
4. Shubayev, V. I.; Pisanic, T. R.; Jin, S. Adv Drug Deliv Rev 2009, 6, 467.
5. Blakemore, R.P. Science 1975, 190, 377.
6. Chen, J. F.; Li, Y.; Wang, Z. F; Li, J. L.; Jiang, W.; Li, S.H. J Integr Plant Biol 2009, 4, 409.
7. Arakaki, A.; Nakazawa, H.; Nemoto, M.; Mori, T.; Matsunaga, T. J R Soc Interface 2008, 26, 977.
8. Christine, D.; Ijeoma, F. U.; Andreas, G.S. Adv Drug Deliv Rev 2005, 57, 2177.
9. Rapoport, M.; Lorberboum-Galski, H. Expert Opin Drug Deliv 2009, 5, 453.
10. Wang, H.; Zhang, S.; Liao, Z.; Wang, C.; Liu, Y.; Feng, S.; Jiang, X.; Chang, J. Biomaterials 2010, 25, 6589.
11. Lee, J.; Tung, C. H.; Anna, M.; Ralph, W. Bioconjugate Chem 1999, 10, 186.
12. Dailey, L. A.; Kleemann, E.; Merdan, T.; Petersen, H.; Schmehl, T.; Gessler, T.; Hänze, J.; Seeger, W.; Kissel, T. J Control Release 2004, 100, 425.
13. Godbey, W. T.; Barry, M. A.; Saggau, K. K.; Kenneth, K. W.; Kenneth, G. M. J Biomed Mater Res 2000, 51, 321.
14. Zhang, W.; Chen, Z.; Song, X.; Si, J.; Tang, G. Technol Cancer Res Treat 2008, 7, 103.
15. Yuan, X. B.; Li, H.; Yuan, Y. B. Carbohydr Polym 2006, 65, 337.
16. Banerjee, T.; Mitra, S.; Singh, A. K.; Rakesh, K. S.; Maitra, A. Int J Pharm 2002, 243, 93.
17. Lewin, M.; Carlesso, N.; Tung, C. H.; Tang, X. W.; Cory, D.; Scadden, D. T.; Weissleder, R. Nat Biotechnol 2000, 18, 410.
18. Zhao, M.; Kircher, M. F.; Josephson, L.; Ralph, W. Bioconjugate Chem 2002, 13, 840.
19. Tueng, S.; Ralph, W.; Mikhail, P.; Alexei, B.; Thomas, J. B. Magn Reson Med 1993, 29, 599.
20. Rudolf, H.; Robert, H.; Matthias, Z.; Dirk, S.; Udo, H.; Ingrid, H.; Werner, A. K. J Magn Magn Mater 2005, 293, 80.
21. Pan, B. F.; Gao, F.; Gu, H. C. J Colloid Interface Sci 2005, 284, 1.
22. Pan, B.; Cui, D.; Sheng, Y.; Ozkan, C.; Gao, F.; He, R.; Li, Q.; Xu, P.; Huang, T. Cancer Res 2007, 67, 8156.
23. Lei, H.; Shuangyan, L.; Yong, Y.; Fengmei, Z.; Jie, H.; Jin, C. J Magn Magn Mater 2007, 313, 236.
24. Petersen, H.; Merdan, T.; Kunath, K. D.; Fischer, D.; Kissel, T. Bioconjugate Chem 2002, 13, 812.
25. Kleemann, E.; Neu, M.; Jekel, N.; Fink, L.; Schmehl, T.; Gessler, T.; Seeger, W.; Kissel, T. J Control Release 2005, 109, 299.
26. Tandon, V.; Kirby, B. J Electrophoresis 2008, 29, 1102.
27. Halama, A.; Kulinski, M; Librowski, T; Lochynski, S. Pharmacol Rep 2009, 6, 993.
28. Scherer, F.; Anton, M.; Schillinger, U.; Henke, J.; Bergemann, C.; Krüger, A. Gene Ther 2002, 9, 102.
29. Choi, J. S.; Nam, K.; Park, J. Y.; Kim, J. B.; Lee, J. K.; Park, J. S. J Control Release 2004, 99, 445.
30. Vladimir, P. T.; Ram, R.; Volkmar, W.; Tatyana, S. L. Proc Natl Acad Sci 2001, 98, 8786.
31. Prochiantz, A. Curr Opin Cell Biol 2000, 12, 400.
32. Han, L.; Zhang, A.; Wang, H.; Pu, P.; Jiang, X.; Kang, C.; Chang, J. Hum Gene Ther 2010, 4, 417.
33. Santra, S.; Yang, H.; Stanley, J. T.; Holloway, P.; H; Moudgil, B. M.; Walter, G.; Mericle, R. A. Chem Commun 2005, 25, 3144.